ORIGINAL ARTICLE

Landslide susceptibility assessment in mountainous area: a case study of Sichuan–Tibet railway, China

Ruian Wu[1] · Yongshuang Zhang[2] · Changbao Guo[1] · Zhihua Yang[1] · Jie Tang[3] · Fangrui Su[3]

Abstract

In the southeastern Tibetan Plateau with complex geological conditions, the frequent and disastrous geological hazards have posed a severe challenge to the construction and operation safety of the planning Sichuan–Tibet railway. Based on the remote sensing and field investigation, the detailed landslide inventory of Jiacha–Langxian segment of Sichuan–Tibet railway was established. After analyzing the general development characteristics of landslides, a total of seven causative variables were selected as input parameters to evaluate landslide susceptibility using the weight of the evidence model. Combined with the probability prediction map and field validation, the landslide susceptibility was classified into four categories: very high, high, moderate and low susceptibility. Based on the landslide susceptibility assessment map, the very high and high susceptibility zones are mainly distributed on the both sides of the Yarlung Zangbo river and its tributaries, and the moderate and low susceptibility zones are located 5 km north to the river. Considering the terrain and landslide disaster prone situation in this region, the planning railway line in tunnel on the north bank of the Yarlung Zangbo river is considered to be reasonable. As for the subgrade and bridge section of the railway, especially for tunnel entrance, necessary slope reinforcement should be carried out. Considering the objective safety threat from landslides to the railway, we hold the opinion that it is necessary to compare the scheme of changing route and taking engineering protection measures in the Langzhen–Langxian segment.

Keywords Landslide susceptibility · GIS · Weight of evidence · Sichuan–Tibet railway · Tibetan plateau

Introduction

It is a complex and systematic scientific work to carry out railway planning and construction in an active tectonic zone as well as the mountainous area (Huang et al. 2013; Zhang et al. 2017; Laimer 2017). Geological environment conditions are important factors that restrict and affect project planning. Landslide, as a kind of the most common geological disasters in mountainous areas, often brings great economic and human losses, which is an unavoidable problem in the process of project planning and construction (Sarro et al. 2018;

Kumar et al. 2019). To reduce and manage landslide-related disasters, it is important to assess landslides susceptible areas for providing references for railway planning (Macciotta et al. 2016; Mehebub and Haroon 2017). The planning area from Jiacha to Langxian of the proposed Sichuan–Tibet railway line is located in the southeast Tibetan Plateau, which is one of the landslide-prone zones in China (Wu et al. 2017; Du et al. 2019). In general, the unstable slopes may be avoided or stabilized in selecting railway line. Some potential unstable slopes have not significantly failed at present, but they are likely to slide in the future. In terms of construction difficulty and operation safety, geological conditions including the development status and trend of geological hazards are very important issues for railway line selection in mountainous area (Laimer 2017). Hence, it is necessary and meaningful to delineate the landslide-prone zones for the proposed railway route so that the effective disaster prevention and mitigation measures can be adopted to reduce losses.

Landslide susceptibility refers to the probability of the spatial occurrence of a landslide given a set of geological environmental conditions, showing the control effect of

✉ Yongshuang Zhang
zhys100@hotmail.com

1 Institute of Geomechanics, Chinese Academy of Geological Sciences, Beijing 100081, China

2 Institute of Hydrogeology and Environmental Geology, Chinese Academy of Geological Sciences, Shijiazhuang 050061, China

3 China University of Geosciences (Beijing), Beijing 100083, China

the basic property of geological environment on landslide (Pandey et al. 2019). Nowadays landslide susceptibility mapping becomes a useful tool in land use and landslide risk management (Gorsevski et al. 2006). With the rapid development of geographic information system (GIS) and remote sensing (RS) techniques in past few years, several different approaches based on GIS have been used to evaluate landslide susceptibility involving qualitative or quantitative methods by different scholars. Qualitative methods rely on expert opinions, and quantitative approaches focus on studying the relationship between causative factors and landslides. Literature survey shows that numerous research and analysis approaches are proposed for landslide susceptibility evaluation, i.e., analytic hierarchy process (AHP) (Barredo et al. 2000), weighted linear combination (WLC) (Ayalew et al. 2004), bivariate statistics (Guzzetti et al. 1999; Thiery et al. 2007), multivariate statistics (Lee et al. 2008), logistic regression (Dai and Lee 2003; Duman et al. 2006; Chauhan et al. 2010; Akgun 2012), frequency ratio (Lee and Pradhan 2006, 2007; Yilmaz 2010; Akinci et al. 2011), certainty factor method (Binaghi et al. 1998; Lan et al. 2004; Sujatha et al. 2012), and weight of evidence model (WOE) (Lee et al. 2004; Tangestani 2009; Park 2011; Armas 2012; Neuhauser et al. 2012; Thiery et al. 2014; Saponaro et al. 2015), etc. Of course, the approaches proposed in the literature are far more than these (Lee et al. 2004; Champati Ray et al. 2006; Akgun 2012; Tien Bui et al. 2012; Pradhan 2013; Youssef et al. 2016; Sciarra et al. 2017). However, no agreement has been reached on the analysis methods used for mapping landslides susceptibility. The purpose of this paper is to analyze the general development and distribution characteristics of the existing landslides, assess the most important conditioning factors for landslides in an active tectonic zone as well as mountainous area and delineate the landslide-prone zones in the study area using the WOE model which is a very popular method and suitable for active tectonic zone as well as mountain areas.

Geological setting

The study area is located in the middle reaches of the Yarlung Zangbo river, low-lying east to the west. The study is focused in an area of 1691 km² which lies within the latitude 29° 00′ N–29° 12′ N and longitude 93° 30′ E–93° 15′ E (Fig. 1). The average elevation of the mountain tops on both sides of the valley is more than 5000 m, and the regional average elevation is about 4100 m, characterized by mountains, wide valleys and canyons. Terraces are developed in the river's convex bank, while bedrocks are exposed in the concave bank. Due to high altitude, cold weather and temperature changes, the rocks of high elevation areas are extremely fragmentized resulting from strong freezing weathering, especially the areas near the snowline. Glacial erosion geomorphology is also developed in the study area. Vertical river incisions steepen the hill slope on both sides of the river which decrease slope stability.

From a geological point of view, this area lies at the Yarlung Zangbo river suture zone between Himalayan plates in the south and Gangdise-Nyainqentanglha plate in the north (Sun and Wang 2011). The neotectonic movements in the study area have the characteristics of intermittent uplift in a large area, which can lead to unstability of the earth's surface. The Yarlung Zangbo Fault (YZF) with frequent historical earthquakes runs through this area roughly in EW orientation and tends to dip in south characterizing with thrust movement. Besides, there are a few faults with the direction in NNE developing in the area. Many earthquakes with Ms ≥ 7.0 occurred within the YZF zone in history, i.e., Ms 7.0 earthquake nearby Sangri County in 1915 (Shao et al. 2008), Ms 7.0 earthquake nearby Longzi County in 1947 (Shao et al. 2008), and Ms 7.7 earthquake in the southeast of Langxian (Li et al. 2014).

Based on the geological map, previous studies and field observation, the bedrock exposure in the area is dominated by Mesozoic and Cenozoic strata. The main strata are listed as follows: (a) metamorphic sandstones and siltstones, sericite phyllites, schist formations in the upper Triassic; (b) Jurassic strata consisting of volcanic rocks, limestones, sandstone and argillites; (c) conglomerate and sandstone in the Paleogene; (d) Quaternary sediments that consist of fluvial, alluvial and colluvium deposits.

The climate is temperate and sub-humid, and annual sunshine time can reach 2864 h in the study area. The average annual temperature during the period 1993–2002 is 9.4 °C. July is the warmest month with an average temperature of 16.6 °C, and January is the coldest month with 0.5 °C on average. The mean annual temperature is 9.4 °C, and the temperature fluctuations are large between day and night. Most rocks in this study area have undergone severe weathering. The annual average rainfall is 509 mm according to the statistical data of recent 10 years. Precipitation is usually intense and concentrated during the monsoon from April to September. Abundant rainfall and ice-melt water flow into strongly fractured rocks and loose deposits to reduce slope stability, even trigger landslides.

The Tibetan Plateau uplifting rapidly, coupled with complex folding and faulting of the region, as well as river incision, landslides and weathering activities dominate the regional geomorphic features (Du et al. 2017). The poor conditions include soft or fractured rock mass and intense tectonic activities, severe human engineering activities and adverse climate, which increases the landslide susceptibility. As a result of increasing human construction activities, landslide occurrences become more frequent than before. In August 1998, a landslide occurred in Lasui town, Jiacha
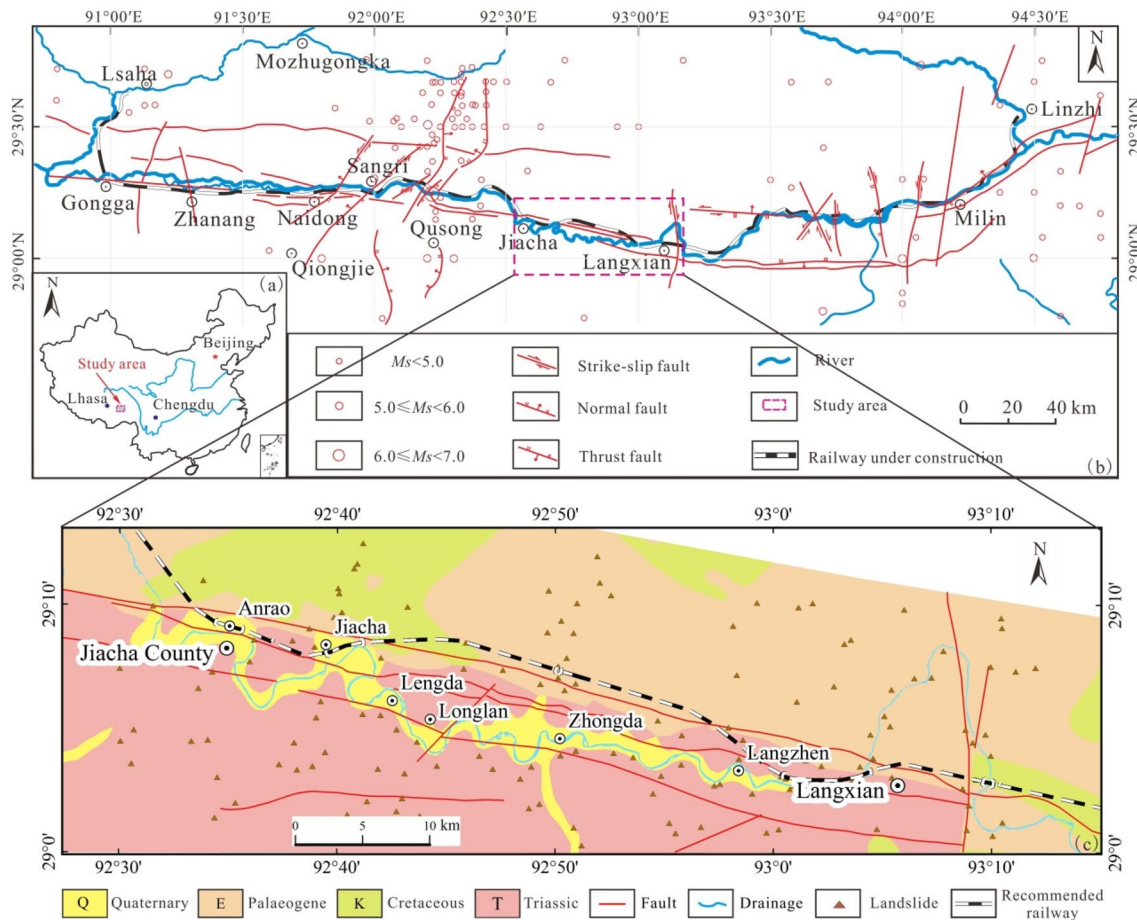
Fig. 1 Geological settings and landslide distribution overview in the Jiacha–Langxian segment of Sichuan–Tibet railway. **a** Geotectonic settings; **b** geographical location and tectonic settings; **c** landslide distribution map

County, which destroyed a road and blocked the traffic for more than 10 days. In August 2001, a slope appeared large deformation in Qizi village of Langxian, and threatened 46 lives of 8 families. Donggeshan landslide in Langxian reactivated in a large scale in 2002 and 2006, and destroyed provincial highway S306 several times. There are some similar landslide cases in this region, and most of the landslides have seriously affected railway planning and construction.

Data and methodology

Landslide inventory

The first step is to acquire information about the landslides that have occurred in the past. This stage is considered as the fundamental part of the landslide studies (Guzzetti et al. 1999; Devkota et al. 2013). Since landslide occurrences in the past and present are keys to spatial prediction in future (Guzzetti et al. 1999), the construction of a landslide inventory map and obtaining the relationship between landslides

and causative factors is essential for landslide susceptibility. Because of the high elevation, difficult access and poor working conditions in the Tibet, landslides are poorly studied, particularly in the deeply incised valleys in the southeast of Tibetan Plateau. Based on data collection, extensive field investigation and aerial photograph interpretation, a total of 157 landslide events in the study area were mapped at 1:50,000 scale and subsequently digitized for further analysis. On the basis of collecting geological hazards data before 2004, some landslides were interpreted from the high-resolution satellite images from Google Earth obtained from 2005 to 2015, and SPOT-5 satellite (ground resolution of 10 m) obtained in 2010. Then, the field landslide investigation and verification were conducted in 2015. Recent landslides were identified using breaks in the forest canopy, bare soil, or other geomorphic characteristics such as head and side scarps, flow tracks, and soil and debris deposits below a scar (Lee and Pradhan 2007). The attribute data of a landslide includes area, perimeter, volume, length, width, type, activity, position on the hillslope, vegetation, main causes, damage, and so on (Regmi et al 2010). The

mapped landslides were distributed in an area of 69.33×10^6 m^2. The individual landslide area ranged from 1274.1 m^2 to 2.95×10^6 m^2.

Based on the field investigation and spatial analysis, the relationship between landslide distribution characteristics and geological factors was obtained. The major landslide type was soil slide (Varnes 1978) in the study area. Most of them were medium to minor in scale. Soil slides accounted for 84% of the landslides and sliding materials were mainly loose colluvium, slide debris and residual deposits. The rest rock slides were mainly developing in weak strata such as phyllites, slates and fractured rock mass near the fault. Most landslides developed on both sides of Yarlung Zangbo river and its tributaries, which was closely related to the control effect of river erosion in slope toe. The amount of landslides whose volume exceeded 1 million m^3 accounted for 25% of all landslides. Some landslides were run through by faults with large angle intersecting in the sliding direction (Fig. 2a). There were also many landslides, whose sliding directions were parallel to the fault, and some faults can even form landslides boundary (Fig. 2b); several giant ancient rock slides were found in the YFZ, and some ancient landslides have reactivated under the influences of slope toe excavation or intense rainfall (Fig. 2c).

WOE model

The weight of evidence method (WOE) is a data-driven quantitative approach, and it assumes that future landslides will occur under the similar or same conditions to those contributing to past comparable landslides in the same type. In the WOE method, the absence or presence of instability has the same significance. It also assumes that causative factors for the mapped landslides remain constant over time (Regmi et al. 2010). Meanwhile, it assumes conditional independency among the landslide impact factors. Though the WOE method is limited to the assumption on conditional independence, it is not constrained by the classical assumptions of the parametric methods, such as distribution assumptions which spatial data often violate, and the method can often provide results easy to explain (Ilia and Tsangaratos 2016). The features make the WOE model stand out from other
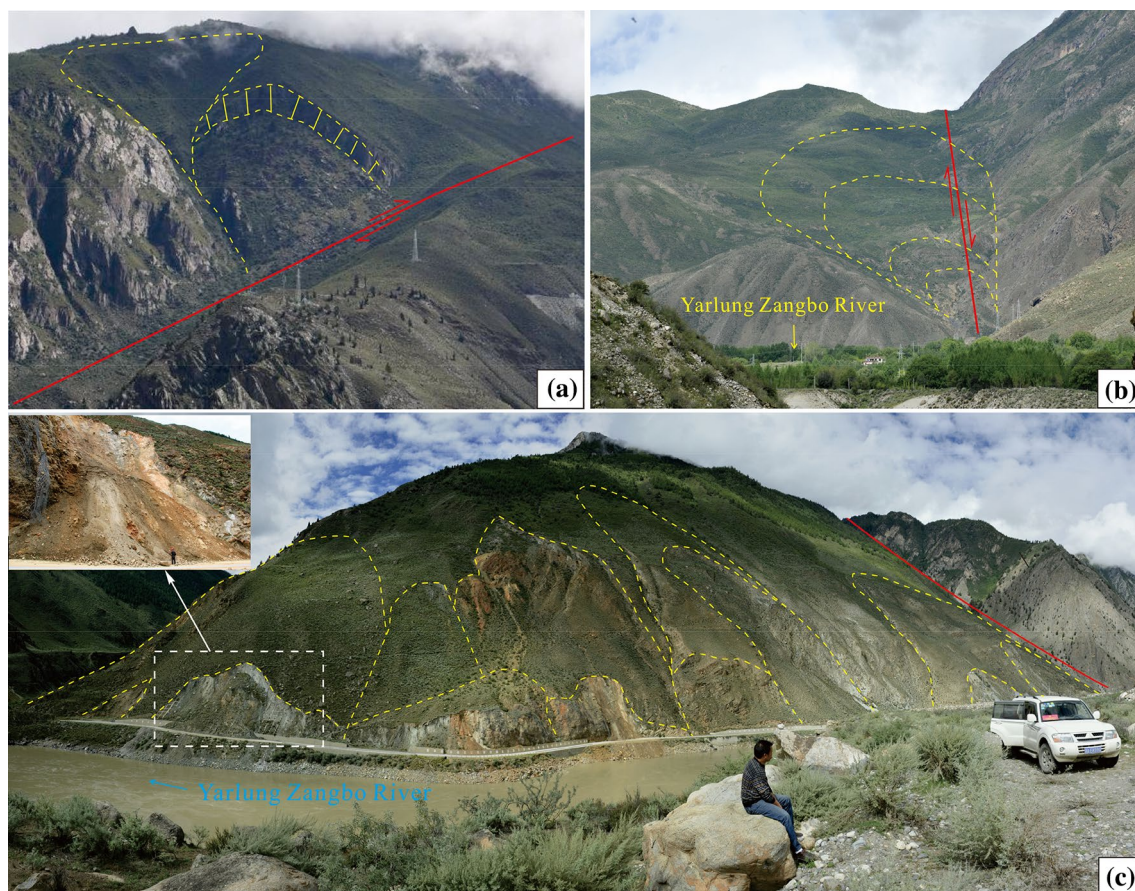

Fig. 2 Typical landslide cases in the study area. **a** A secondary fault run through the front of landslide in the east of Langxian (mirror NE); **b** the sliding direction of Redui landslide is parallel to the YZF (mirror NE); **c** Bajitang landslide group distributed linearly along the Yarlung Zangbo river (mirror SW)

data-driven methods, and the model has been utilized for spatial predictions and landslide susceptibility assessment in numerous studies (van Westen et al. 2003; Lee and Choi 2004; Dahal et al. 2008; Kayastha et al. 2012; Armas 2012; Thiery et al. 2014; Ilia and Tsangaratos 2016). The model is based on Bayes rule and on the concepts of prior and posterior probability. Bonham-Carter et al. (1989) indicated detailed mathematical formulas related to the method which could calculate the contribution of each causative factor on landslide event occurrence. The related equations are listed below:

$$P(A|B) = \frac{P(B|A) \times P(A)}{P(B)}, \tag{1}$$

$$W_i^+ = \ln\left(\frac{P\{B|L\}}{P\{B|\overline{L}\}}\right) = \ln\left(\frac{P(B \cap L)/P(L)}{P(B \cap \overline{L})/P(\overline{L})}\right)$$
$$= \ln\left(\frac{\frac{\text{Landslide area in the considered class}}{\text{Total landslide area}}}{\frac{\text{Stable area in the considered class}}{\text{Total stable area}}}\right), \tag{2}$$

$$W_i^- = \ln\left(\frac{P\{\overline{B}|L\}}{P\{\overline{B}|\overline{L}\}}\right) = \ln\left(\frac{P(\overline{B} \cap L)/P(L)}{P(\overline{B} \cap \overline{L})/P(\overline{L})}\right)$$
$$= \ln\left(\frac{\frac{\text{Total landslide area in the other classes}}{\text{Total landslide area}}}{\frac{\text{Total stable area in the other classes}}{\text{Total stable area}}}\right) \tag{3}$$

$$W_f = W_i^+ - W_i^-. \tag{4}$$

In Eq. (1), $P(A|B)$, states that the probability of some event A occurring when event B has already occurred, which is equal to the probability of event B occurring given that event A has occurred, $P(B|A)$, multiplied by the probability of event A occurring, $P(A)$, and divided by the probability of event B occurring, $P(B)$. This method calculates the weight for each landslide predictive factor (B) based on the presence or absence of the landslide (L) within the area (Bonham-Carter 1994; Guo et al. 2015).

Where ln represents natural log, P indicates the probability, L represents the presence of a landslide, while B is the presence of a causative factor. The bar above a letter indicates the negation. $P\{B|L\}$ represents the probability of B occurring given the presence of L. W_i^+ and W_i^- can be calculated in Eqs. (2) and (3). W_i^+ indicates the probability of landslide occurrence under the action of a predicating factor at the current level. W_i^- indicates the absence of the predicate factor. When $W_i^+ > 0$ or $W_i^- < 0$, it means that the causative factor is positively correlated with the incidence of landslides. When $W_i^+ < 0$ or $W_i^- > 0$, it means the causative factor is negatively correlated with landslide occurrence.

The difference between the two weights is known as the weight contrast. W_f in Eq. (4), reflects the weight of landslide occurrence under the level of the causative factor. The difference between W_f values offers a measure of the magnitude of the correlation between predictor variables and landslides. More detailed descriptions about the meaning of equations above can be seen in other literatures (Bonham-Carter et al. 1989, 1994; Mohammady et al. 2012). After calculating the weight of each variable, they can be added up to make a posterior logit when all variables are conditionally independent.

Landslide causative factors analysis

Previous research has shown that landslide occurrence is an integrated result governed by some causative factors, i.e. topography, tectonic activities, lithology, slope structure, rainfall, underground water, human engineering activities, etc. (Dahal et al. 2008; Sarkar et al. 2008; Yalcin et al. 2011; Bui et al. 2011; Neuhauser et al. 2012; Guo et al. 2015; Ilia and Tsangaratos 2016). Due to lacking of strict criterion for choosing evaluation factor, different factors were selected for assessing landslide susceptibility in different regions. The number of evaluation factors varied from several to more than a dozen. Dahal et al. (2008) selected eight variables such as slope direction, distance from rivers, land use and distance from roads, etc. Ilia and Tsangaratos (2016) chose lithology, elevation, slope, slope direction and distance from roads. Guo et al. (2015) conducted a study on landslide susceptibility along the Xianshuihe fault zone in western Sichuan, China, and discussed the assessment results of selecting 6, 8 and 11 evaluation factors, which showed that the assessment results with more variables were not always better. The accuracy of landslide susceptibility assessment results in the WOE method was determined by the quality of landslide data and the independence of evaluation factors.

According to field investigation and previous research results (Zhou 2011; Wu et al. 2017), these slope failures from Jiacha to Langxian were related to geological, topographical, climatic conditions, tectonic activities, stream erosion, and human engineering activities. These causative variables, topography, lithology, distance to road, distance to stream and the distance from tectonic structures are most often selected as conditioning factors for landslide susceptibility assessment in an active tectonic zone as well as mountainous area (Bui et al. 2011; Neuhauser et al. 2012; Guo et al. 2015; Ilia and Tsangaratos 2016). In general, landslide susceptibility assessment mainly emphasizes the factors in the tendency of landslide under the action of static conditions, which are topography, lithology, tectonic activities.

However, this research only considers the static conditions regarding landslide susceptibility assessment other than external factors such as time, rainfall, earthquakes and human engineering activities. In addition, the roads in study area are built along the rivers, so the distance to river not the distance to road was selected as a conditioning factor. In this research, using bivariate statistics, the assumption is made that all landslides in a given study area occur under the same combination of parameters and that all sets of parameters are conditionally independent (Xu et al. 2012; Guo et al. 2015). Thus, this research takes seven causative factors into account, which are slope degree, slope aspect, elevation, planform curvature, lithology, distance from active faults and distance from rivers (Fig. 3). The relationship between each variable and landslides is studied as follows (Table 1).

Topography

Topography conditions are basic intrinsic factors for landslide occurrence. There is no doubt that the geometric shape of a slope has a certain influence on its stability. In this study, slope angle, slope aspect, slope altitude and planform curvature are considered to analyze the relationship between landslide occurrence and topography. The corresponding maps of the study area are derived from the DEM with cell size 25 × 25 m.

Slope gradient

Slope gradient is one of the most important factors that influence slope stability (Bednarik et al. 2010), which not only affects the stress distribution inside the slope but also affects weathering layer depth and slope surface runoff (Duo et al. 2017). The slope angles of this area ranged from 0° to 78°, which were divided into five categories: 0°–10°, 11°–20°, 21°–30°, 31°–40°, and > 40°. The thematic data layer and statistical results of landslide occurrence with each slope angle class were presented in Fig. 4a and Table 1.

Slope aspect

Different slope aspects will lead to different slope conditions, i.e. weathering, precipitation, snowmelt water, vegetation cover, soil infiltration, etc. Furthermore, influenced by the movement of the upper wall of the thrust fault, the occurrence probability of landslides on different aspects were different (Huang and Li 2008). Slope aspects of this area were classified into nine categories, namely, N, NE, E, SE, S, SW, W, NW and flat. The related thematic data layer was shown in Fig. 4b.

Altitude

Altitude is a good indicator of landslide occurrence (Duman et al. 2006). The altitude of this area ranged from 3026 to 5512 m, which can be divided into five categories (Fig. 4c, Table 1): < 3500 m, 3500–4000 m, 4001–4500 m, 4501–5000 m, > 5000 m.

Planform curvature

Planform curvature refers to the fluctuation degree of the convex or concave on the slope surface. A positive value represents that the surface is laterally convex in profile, while a negative value indicates the surface is laterally concave, the value near or at zero means the slope surface is flat. Planform curvature reflects the surface roughness, fluctuation, the capability of soils water convergence and divergence which may influence landslide stability because of changing the erosion process and soil moisture content. In addition, the geological materials located at uneven part of a slope may be easily damaged under seismic load. Three classes (concave, convex, plan) were identified in this study (Fig. 4d, Table 1).

Distance to fault

The fault zones are considered as poor geological areas due to the fractured rock mass structure and soils with high permeability. The probability of a landslide event increases in the areas near fault zones (Kanungo et al. 2006; Ilia and Tsangaratos 2016). It is accepted that faults would affect landslide occurrence with distance up to few kilometers. The faults were digitized from the scale 1: 200,000 geological map. The fault buffer map (Fig. 4e) about the distances of grids to each fault was prepared and classified into five different buffer zones, namely, < 1000 m, 1001–2000 m, 2001–3000 m, 3001–4000 m, > 4000 m.

Lithology group

Lithology is usually considered as an important causative factor of landslides. The engineering geological properties of rock and soil mass were proposed to partition rock units (Dai et al. 2001). The lithology map was derived from the scale 1:200,000 geological map and field investigation. In the present study, we grouped the lithology units of the area into seven lithological classes, as shown in Tables 1 and 2 and Fig. 4f. Considering that the rocks were severely weathered and fragmented near the YZF due to the tectonic activity, fractured rock masses were classified as a group separately.
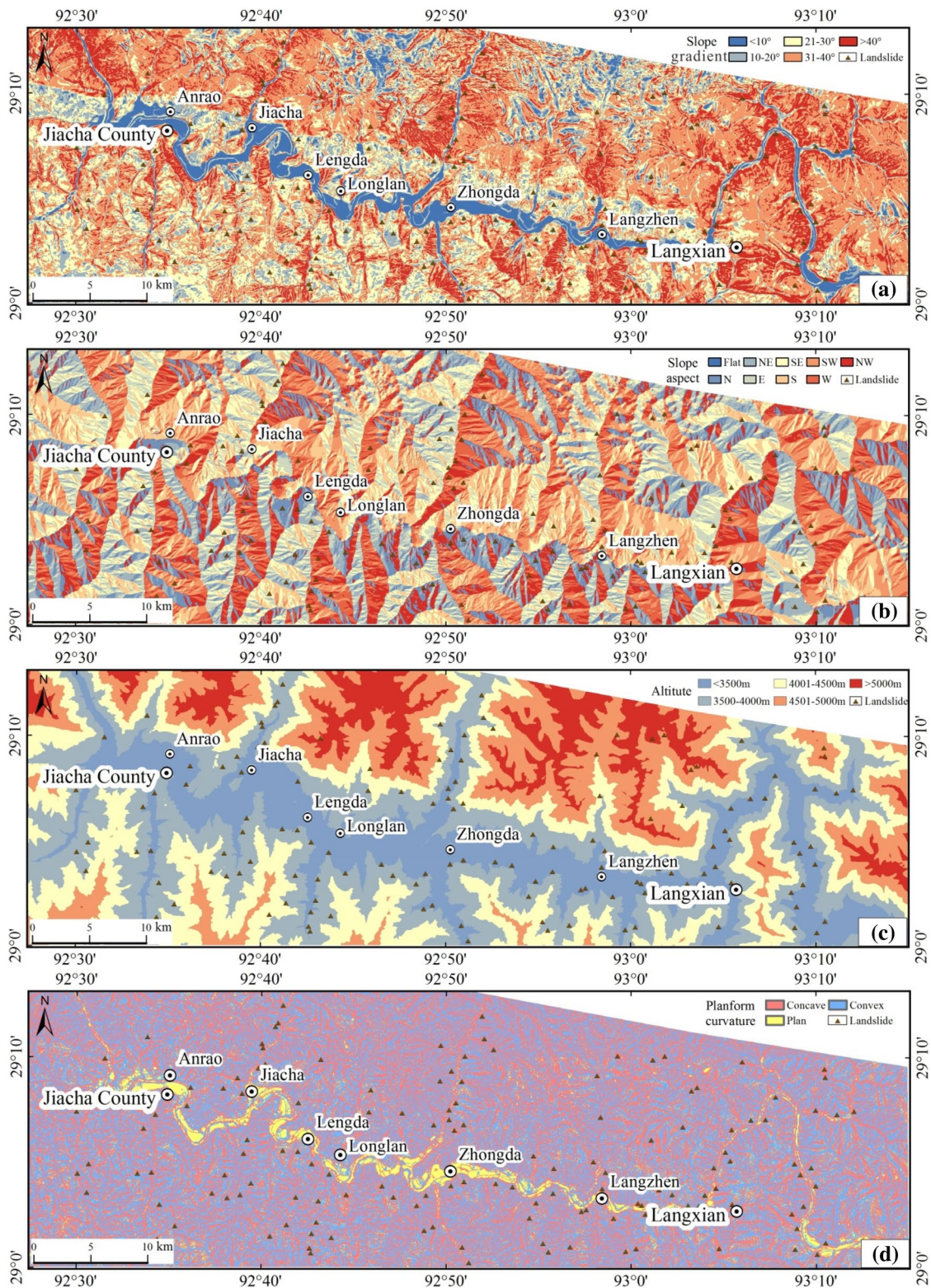
Fig. 3 Thematic maps of landslide causative factors. **a** Slope gradient; **b** slope aspect; **c** altitude; **d** planform curvature; **e** distance to fault; **f** lithology group; **g** distance to river
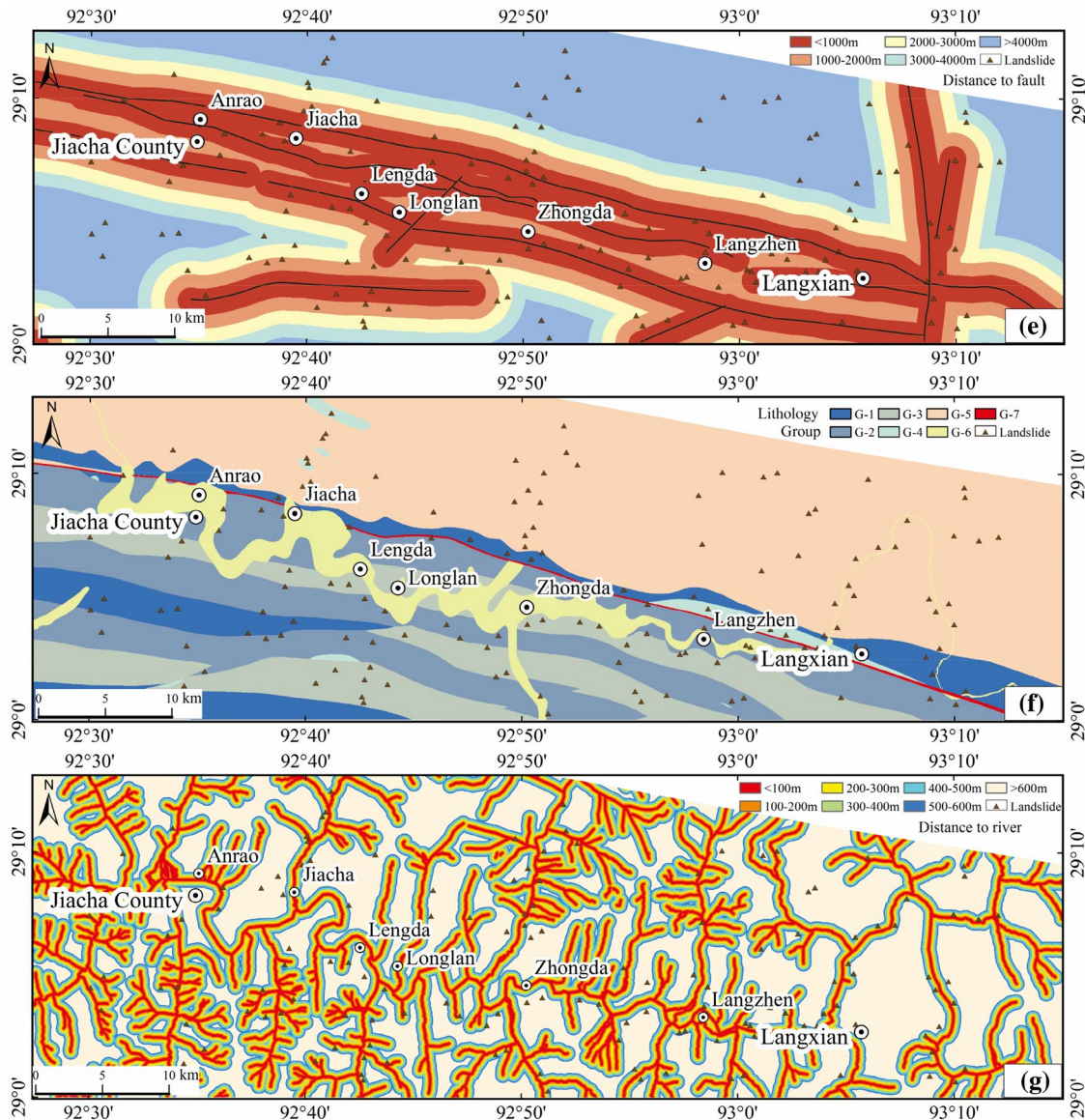
Fig. 3 (continued)

Distance to river

Stream erosion is one of the most important factors that reshape the landform of slopes by the river bank. In addition, slope toe erosion by running water may affect the stability of landslides as high water content in slopes by the river causes the reduction of slope stability. The river buffer map (Fig. 4g) about the distances of grids to each river was prepared and classified into seven different buffer zones, namely, < 100 m, 101–200 m, 201–300 m, 301–400 m, 401–500 m, 501–600 m, > 600 m. The values (Table 1) and map (Fig. 4g) were obtained by analyzing the distance between the sample grid and the nearest river.

Landslide susceptibility assessment results

Landslide susceptibility mapping

In present study, W_{fi} was applied as factor weight in the WOE model, and all W_f values of those variables mentioned above in each grid were summed up to obtain landslide susceptibility index (LSI), which stood for landslide susceptibility. Based on the natural break classifier, the LSI values were divided into four classes, which were very high, high, moderate and low landslide susceptibility. Table 3 showed the percentage of each class, which occupied 16.64%, 29.46%, 31.37% and 22.53%, respectively. The landslide area in the very high and high susceptibility zones took 81.6% of the

Table 1 Weighted information values of landslide causative factors

Factor	Class	Class area from total area (%)	Percentage of land-slides area (%)	Weight W_i^+	Weight W_i^-	W_f
Slope gradient (°)	0–10	7.81	1.74	− 1.5319	0.0664	− 1.5983
	11–20	12.67	17.70	0.3509	− 0.0617	0.4126
	21–30	24.79	36.52	0.4073	− 0.1760	0.5833
	31–40	37.14	30.92	− 0.1902	0.0985	− 0.2887
	> 40	17.59	13.12	− 0.3039	0.0551	− 0.3591
Slope aspect	Flat	0.21	0	− 5.5100	0.0022	− 5.5122
	N	9.90	16.13	0.5150	− 0.0746	0.5896
	NE	11.35	12.24	0.0785	− 0.0105	0.0890
	E	12.16	8.88	− 0.3252	0.0382	− 0.3634
	SE	13.11	12.15	− 0.0786	0.0114	− 0.0899
	S	14.20	12.67	− 0.1178	0.0183	− 0.1362
	SW	13.64	8.87	− 0.4452	0.0561	− 0.5013
	W	13.19	14.54	0.1022	− 0.0164	0.1186
	NW	12.24	14.50	0.1772	− 0.0272	0.2044
Altitude (m)	< 3500	19.25	36.35	0.6737	− 0.2469	0.9206
	3500–4000	29.10	47.62	0.5196	− 0.3137	0.8334
	4001–4500	24.60	10.99	− 0.8291	0.1736	− 1.0028
	4501–5000	18.58	4.15	− 1.5298	0.1706	− 1.7004
	> 5000	8.47	0.88	− 2.2988	0.0831	− 2.3819
Planform curvature	Concave	46.72	46.70	− 0.0003	0.0003	− 0.0006
	Plan	6.45	5.11	− 0.2431	0.0149	− 0.2580
	Convex	46.83	48.19	0.0299	− 0.0270	0.0170
Distance to faults (m)	0–1000	37.42	54.69	0.3974	− 0.3334	0.7308
	1001–2000	20.79	25.29	0.2044	− 0.0606	0.2651
	2001–3000	14.96	11.03	− 0.3151	0.0470	− 0.3621
	3001–4000	10.57	4.75	− 0.8210	0.06558	− 0.8866
	> 4000	16.25	4.25	− 1.3707	0.1396	− 1.5103
Lithology group[a]	G-1	11.16	12.85	0.1473	− 0.0200	0.1673
	G-2	20.22	29.28	0.3889	− 0.1252	0.5141
	G-3	13.84	24.51	0.6041	− 0.1373	0.7414
	G-4	1.26	2.23	0.6060	− 0.0103	0.6163
	G-5	46.27	26.86	− 0.5614	0.3237	− 0.8850
	G-6	6.70	3.14	− 0.7780	0.0390	− 0.8169
	G-7	0.56	1.14	0.7592	− 0.0061	0.7653
Distance to rivers (m)	0–100	12.17	8.93	− 0.3201	0.0377	− 0.3578
	100–200	10.51	12.43	0.1746	− 0.0225	0.1971
	201–300	9.84	12.94	0.2855	− 0.0362	0.3217
	301–400	9.12	12.12	0.2967	− 0.0348	0.3315
	401–500	8.33	10.78	0.2688	− 0.0281	0.2969
	501–600	7.44	9.12	0.2121	− 0.019	0.2311
	> 600	42.56	33.68	− 0.2422	0.1499	− 0.3922

[a]Detailed lithology groups see Table 2

total landslide area. According to Fig. 5, the very high and high landslide susceptibility zones were mainly distributed on both sides of the Yarlung Zangbo river and its tributaries, while the medium and low landslide susceptibility zones were located 5 km north to the river, which was almost accordant with field survey situation.
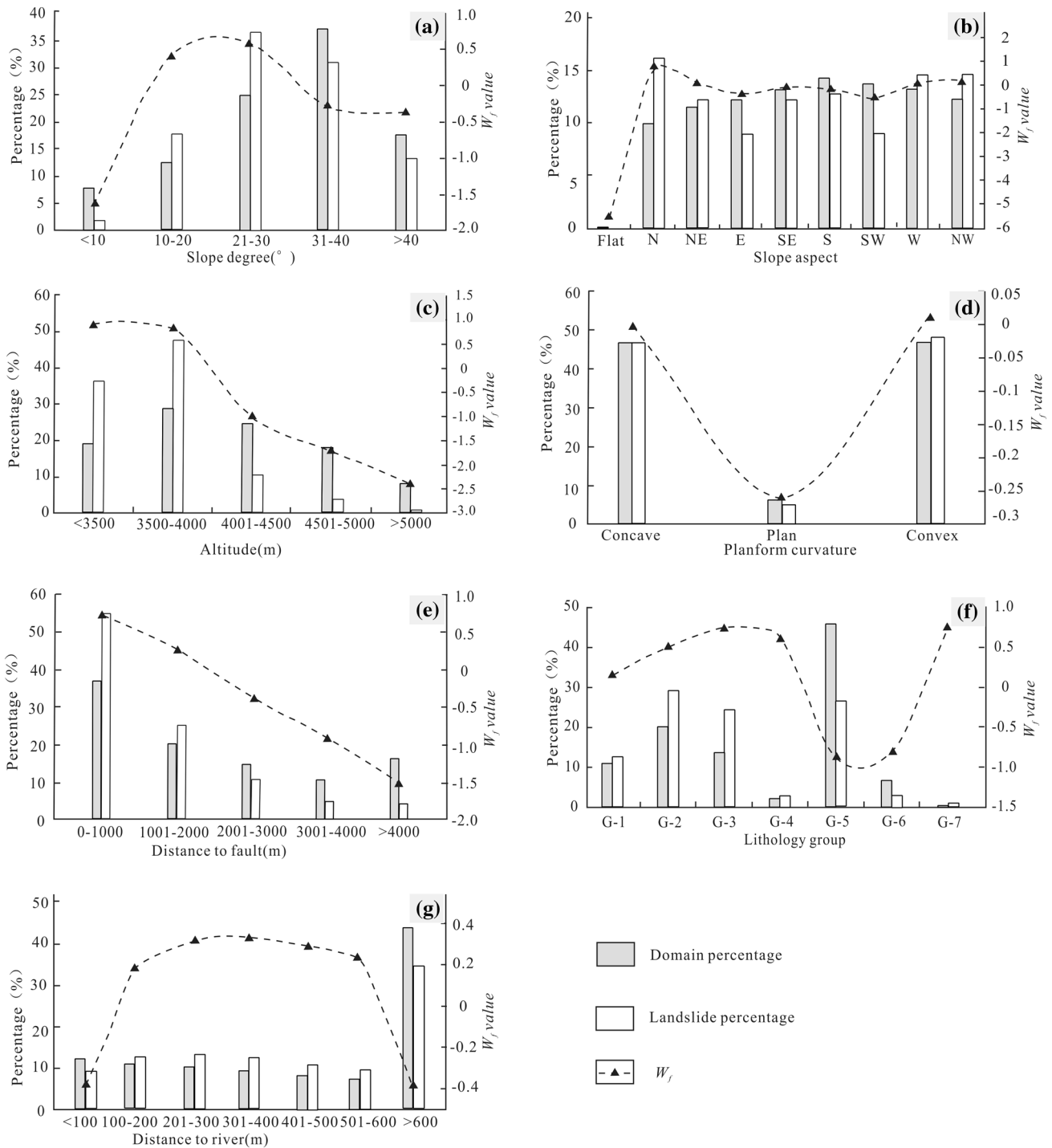
Fig. 4 The statistical relationship between landslide distribution and causative factors

Landslide susceptibility validation

The accuracy of a landslide susceptibility assessment map can be evaluated by various methods, i.e., success rate and prediction rate (Pradhan and Lee 2010). To obtain the success rate curve for the LSI map, the calculated index values of all grids were sorted in descending order. Then, the ordered grid values were categorized into 100 classes with 1% cumulative intervals. The curve plots landslide susceptibility index rank on the *X* axis and the cumulative percentage of landslide occurrence on the *Y* axis. As shown in Fig. 6, the success rate reveals that 10% of study

Table 2 Division of lithology group unit

Lithology group no	Stratum code	Main lithology types
G-1	T_3s, K_1t, K_2sm	Sandstone, argillaceous limestone, mudstone with limestone interbedded
G-2	T_3j, T_3jx, T_3s	Limestone, dolomite with phyllite or slate interbedded
G-3	T_3j, T_3jx, T_3s	Slate, phyllite with metamorphic sandstone interbedded
G-4	Rlb	Polymictic conglomerate, pebbly sandstone, with fine sandstone and siltstone interbedded
G-5	$K_1\gamma\delta$, $K_2\pi$, $(J_3-K_1)s$, K_2m, E_2b, E_2r, E_2x, E_2z	Massive granite, andesite, diorite
G-6	Q_4^{al}, Q_4^{pl}	Clay, gravelly soil, sand, gravel
G-7		Cataclastic rock mass in the fault

Table 3 Statistical results of landslides susceptibility zones in WOE method

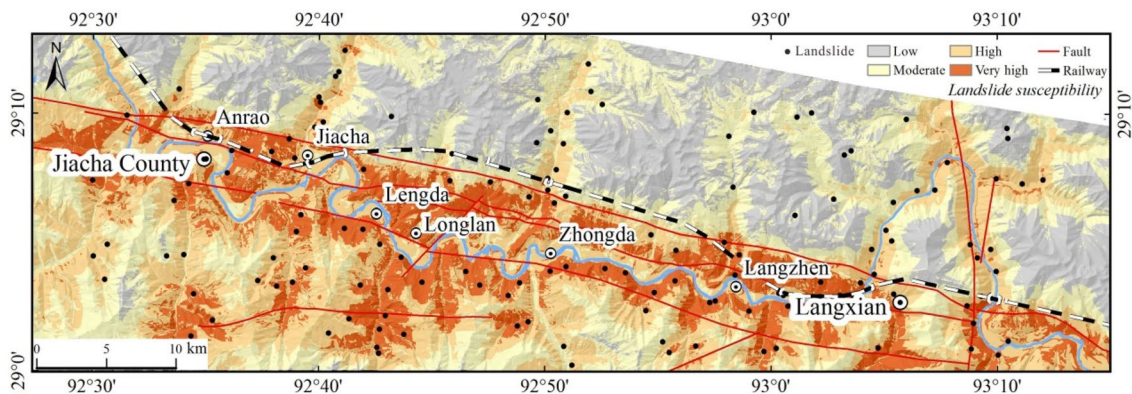| Susceptibility zones	Area (km^2)	Percentage of area (%)	Landslide area (km^2)	Percentage of landslide area (%)
Very high	281.383	16.64	34.924	50.372
High	498.172	29.46	21.679	31.268
Moderate	530.544	31.37	9.428	13.597
Low	381.055	22.53	3.302	4.763

Fig. 5 Landslide susceptibility map obtained by the WOE model

area where LSI had higher values could explain about 35% of total landslides. Likewise, 20% of higher *LSI* values could explain about 53% of all landslides, 30% of higher *LSI* values could explain about 67% of all landslides. In this study, area under the curve of the success rate is 0.813, indicating the success rate is 81.3%, thus the model is valid.

Discussions

Data distribution

In the WOE method, it is assumed the data amount of each factor should obey a normal distribution. According to Bonham-Carter (1994), this ideal but rough assumption may lead to some errors. Non-parametric statistics can be used to solve this problem due to the advantage that they are not on the basis of normal distribution (Ilia and Tsangaratos 2016). In fact, the data amount related to landslide occurrence is hardly normally distributed.
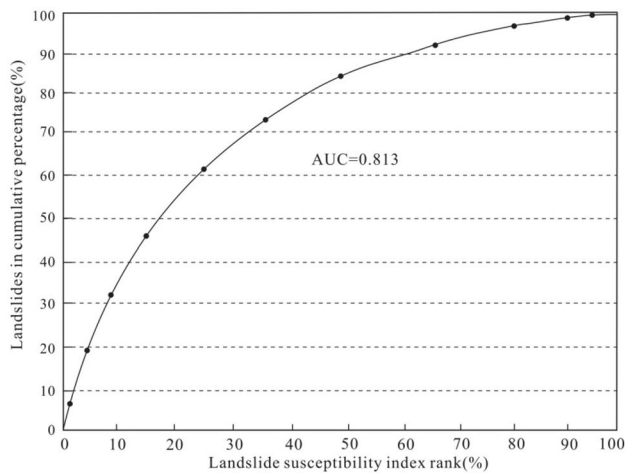
Fig. 6 Success rate curve of landslide susceptibility

In terms of a single factor, most landslides occurred on the slope with angles ranging from 21° to 40°. The largest landslide areas were on the slopes of 21°–30°, few landslides developed on the slopes of 0°–10°, 11°–20° and > 40°. In addition, the area of landslides with N aspect was larger than other aspects. Statistical analysis showed that most landslides occurred in 3501–4000 m elevation range, followed by the elevation below 3500 m. Landslides occurring below 4000 m elevation account for up to 84% of all landslides, because the zones with elevation 3501–4000 m have been affected strongly by unfreezing, and the zones with an elevation below 3500 m were mainly influenced by human activity, where the landslide occurrences were easy to occur. For planform curvature, the slopes are more likely to slide with convex shape. When it comes to lithology, landslides are well developed in cataclasite rock near the fault, followed by phyllites and slates. About 55% of the landslides were 1 km away from faults and nearly 79.8% occurred within 2 km away from faults. When the distances to faults exceeded 2 km, the landslide amount decreased obviously. There were fewer landslides when the distances to the river were less than 100 m or more than 600 m. In the zones 101–600 m away from a river the closer the distance from a river was, a landslide was more likely to be triggered.

Boundary of study area

In the process of landslide susceptibility evaluation, the area boundary is also an important role besides sufficient landslide data, appropriate scale and effective evaluation model. In some literature, the study areas are generally represented by the natural watershed boundaries and geographical boundaries during the landslide susceptibility evaluation, which can produce comparable and reproducible results. The watershed was also taken into account in selecting geometric

study area boundaries because the geometry area was comparatively small, the watershed can be reflected. But, if we focus on the landslide susceptibility in narrow and linear scopes, i.e., fault zones, highways, and their adjacent areas, the geometric boundaries are often selected as study area boundaries (Xu et al. 2012; Regmi et al. 2014; Guo et al. 2015). In this study, the landslide susceptibility of the proposed railway line and its surrounding areas was of great concern. In other words, the area of interest has already been included in the selected geometric boundaries. In fact, the landslide susceptibility evaluation results are proved to be good. So, the selected geometric boundaries can meet current research objectives.

Assessment method about different landslide types

Soil slides and rock slides (Varnes 1978) have occurred predominantly in the study area. In general, when the WOE method is applied to one single type of landslides, it can provide a better landslide susceptibility assessment result than being applied to various types of landslides. Combination of landslide susceptibility maps of different types into a single map would be a good solution, but the combination of two or more maps of weighted values is impossible in the WOE method since the weighted values are not comparable (Regmi et al. 2010). Many scholars have also applied the WOE method in evaluating landslide susceptibility for various types of landslides (Regmi et al. 2010; Xu et al. 2012; Guo et al. 2015). Meanwhile, considering there was a certain correlation between the soil slides and the rock slides, the amount and total volume of rock slides were small relatively, a map showing susceptibility zones to all types of landslides would provide a good choice for the decision makers.

Application of landslide susceptibility assessment results

According to the landslide susceptibility map, we can find the landslide-prone zones with very high and high susceptibility are concentrated on both banks of the Yarlung Zangbo river within the fault zones. Limited to valley topography and threated by landslides occurrence, the line scheme of combing mountain tunnel and bridge-subgrade traversing the study area along the valley is not feasible. At present, the main part of the proposed railway line is suggested to traverse from the north bank of Yarlung Zangbo river in mountain tunnel, and local sections outside the mountain may be connected by roads or bridges (Fig. 5).

As a ground surface disaster, landslide mainly endangers railway safety in forms of destruction and burial. Hence, it is very important to select tunnel entrance carefully and strengthen engineering support in landslide-prone zones. The terrain of the subgrade sections near

Anrao town and Jiacha town (Fig. 7a, b) is flat and widen, and the railway line is relatively far from the landslide zones with high susceptibility, which is less likely to be affected by landslide hazards. In addition, the two sections of the railway near Zhongda town and the great bend of the river in the east of Langxian (Fig. 7c, e) need to cross the valley in the form of bridge. Some tunnel entrances in these four sections of the railway are located in the zones with high landslide susceptibility. Influenced by blasting vibration and excavation disturbance in tunnel construction, some landslides may occur or reactivate. So, we suggest strengthen geotechnical investigations on the slopes at the tunnel entrances. The tunnel entrance positions can be changed, or some effective engineering support measures can be taken if necessary.

The proposed railway line from Langzhen to Langxian section is suggested to traverse along the river valley in subgrade. But the area on the northern side of the railway line is of very high landslide susceptibility, and some large ancient landslides develop there. Landslide could occur once the toes of those ancient landslides are excavated or disturbed during railway construction. Considering the influence of landslide hazards on the railway, this section of railway line should be changed to pass through the mountain in tunnel, as shown in the black dotted line in Fig. 7d. If this section of the railway line is not changed, detailed investigation and stability analysis of the ancient landslides must be carried out, and the disturbance to ancient landslides should be reduced during railway construction as much as possible.

Conclusions

The landslide susceptibility is of great significance for landslide risk management, railway planning, and construction guidance. Based on the detailed remote sensing interpretation and field investigation, a reliable landslide spatial database was created in the Jiacha–Langxian segment of Sichuan–Tibet railway, then which was used to conduct landslide characteristics analysis and landslide susceptibility assessment with the WOE model. Some beneficial conclusions are as follows:

1. The very high and high landslide susceptibility zones are mainly distributed on both sides of the Yarlung Zangbo river and its tributaries, while the moderate and low landslide susceptibility zones are located 5 km north to the river. Topography, lithology, active fault and river erosion play dominant roles in determining landslide development.
2. The main part of the proposed railway line through the north bank of the Yarlung Zangbo river in mountain tunnel is considered as a reasonable route, and the tunnel sections in different mountains can be connected by roads or bridges. Influenced by blasting vibration and excavation disturbance in tunnel construction, some landslides near the tunnel entrances may occur or reactivate. So the tunnel entrance locations should be cautiously selected and the unstable slopes at the tunnel entrance in the landslide-prone zones should be reinforced.
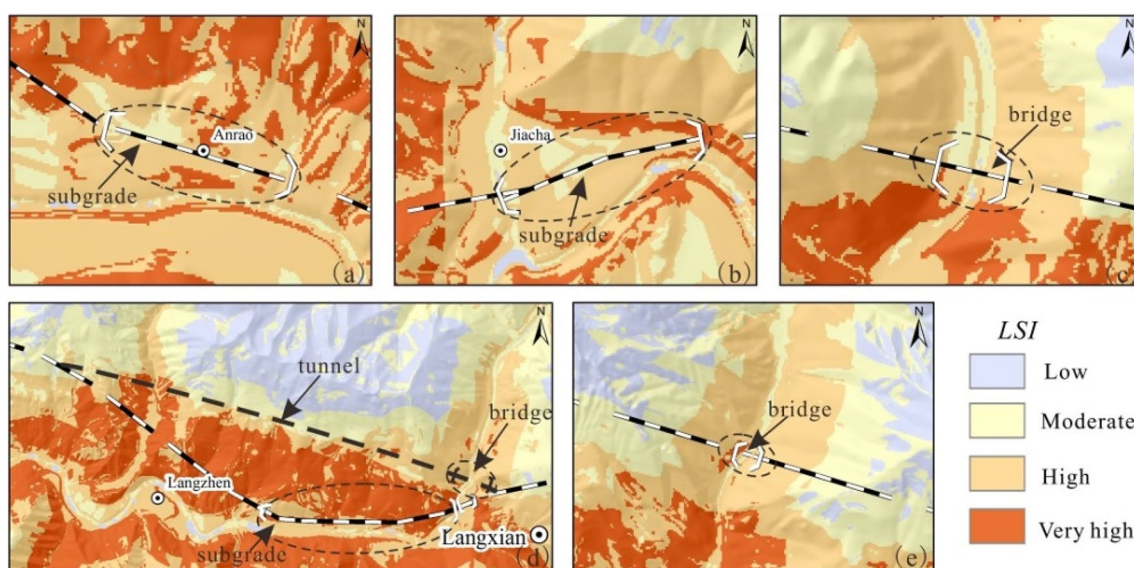

Fig. 7 Relationship between landslide susceptibility zones and the proposed railway line

3. Considering the possible influence of ancient landslide reactivation, the scheme of changing the line from Langzhen to the west of Langxian section should be considered to mitigate the future landslide hazards. This section of the railway can pass through the mountain in tunnel instead of traversing along the river valley in subgrade. If not, the necessary engineering measures must be carried out to improve the stability of the ancient landslides.

4. Though the occurred landslides can be identified, the identification of the slopes which may fail over time under the same causative factors is difficult. Based on the analysis of the present landslide distribution and development characteristics, the relationship between the landslides and causative factors can be found out, and the landslide susceptibility can be established to identify the landslide-prone areas for guiding railway line selection. The presented thought and approach can provide a reference for railway line selection in mountainous areas.

References

Akgun A (2012) A comparison of landslide susceptibility maps produced by logistic regression, multi-criteria decision, and likelihood ratio methods: a case study at İzmir. Turkey Landslides 9(1):93–106

Akinci H, Doğan S, Kilicoğlu C, Temiz MS (2011) Production of landslide susceptibility map of Samsun (Turkey) City Center by using frequency ratio method. Int J Phys Sci 6(5):1015–1025

Armas I (2012) Weight of evidence method for landslide susceptibility mapping. Prahova Subcarpathians, Romania. Nat Hazards 60:937–950

Ayalew L, Yamagishi H, Ugawa N (2004) Landslide susceptibility mapping using GIS-based weighted linear combination, the case in Tsugawa area of Agano River, Niigata Prefecture, Japan. Landslides 1:73–81

Barredo J, Benavides A, Hervás J, van Westen CJ (2000) Comparing heuristic landslide hazard assessment techniques using GIS in the Tirajana basin, Gran Canaria Island, Spain. Int J Appl Earth Obs Geoinf 2(1):9–23

Bednarik M, Magulova B, Matys M, Marschalko M (2010) Landslide susceptibility assessment of the Kralovany–Liptovsky Mikulas railway case study. Phys Chem Earth Parts A B C 35(3–5):162–171

Binaghi E, Luzi L, Madella P (1998) Slope instability zonation: a comparison between certainty factor and fuzzy Dempster–Shafer approaches. Nat Hazards 17:77–97

Bonham-Carter GF (1994) Geographic information systems for geoscientists: modelling with GIS, vol 13, computer methods in the geosciences. Pergamon Press, Oxford, p 398

Bonham-Carter GF, Agterberg FP, Wright DF (1989) Weights of evidence modelling: a new approach to mapping mineral potential. In: Agterberg FP, Bonham-Carter GF (eds) Statistical applications in the earth science. Geological survey of Canada, Ottawa, pp 171–183

Bui DT, Lofman O, Revhaug I, Dick O (2011) Landslide susceptibility analysis in the Hoa Binh province of Vietnam using statistical index and logistic regression. Nat Hazards 59(3):1413–1444

Champati Ray PK, Dimri S, Lakhera RC, Sati S (2006) Fuzzy-based method for landslide hazard assessment in active seismic zone of Himalaya. Landslides 4(2):101–111

Chauhan S, Sharma M, Arora MK (2010) Landslide susceptibility zonation of the Chamoli region, Garhwal Himalayas, using logistic regression model. Landslides 7(4):411–423

Dahal RK, Hasegawa S, Nonomura A, Yamanaka M, Dhakal S, Paudyal P (2008) Predictive modelling of rainfall-induced landslide hazard in the Lesser Himalaya of Nepal based on weights-of-evidence. Geomorphology 102(3):496–510

Dai FC, Lee CF (2003) A spatiotemporal probabilistic modelling of storm-induced shallow landsliding using aerial photographs and logistic regression. Earth Surf Process Landf 28(5):527–545

Dai FC, Lee CF, Li J, Xu ZW (2001) Assessment of landslide susceptibility on the natural terrain of Lantau Island, Hong Kong. Environ Geol 40:381–391

Devkota KC, Regmi AD, Pourghasemi HR, Yoshida K, Pradhan B, Ryu IC, Dhital MR, Althuwaynee OF (2013) Landslide susceptibility mapping using certainty factor, index of entropy and logistic regression models in GIS and their comparison at Mugling-Narayanghat road section in Nepal Himalaya. Nat Hazards 65(1):135–165

Du GL, Zhang YS, Iqbal J, Yang ZH, Yao X (2017) Landslide susceptibility mapping using an integrated model of information value method and logistic regression in the Bailongjiang watershed, Gansu Province. China J Mt Sci 14(2):249–268

Du G, Zhang Y, Yang Z, Guo C, Yao X, Sun D (2019) Landslide susceptibility mapping in the region of eastern Himalayan syntaxis, Tibetan Plateau, China: a comparison between analytical hierarchy process information value and logistic regression-information value methods. Bull Eng Geol Environ 78(6):4201–4215

Duman TY, Can T, Gokceoglu C, Nefeslioglu HA, Sonmez H (2006) Application of logistic regression for landslide susceptibility zoning of Cekmece Area, Istanbul. Turk Environ Geol 51(2):241–256

Gorsevski PV, Gessler PE, Boll J, Elliot WJ, Foltz RB (2006) Spatially and temporally distributed modeling of landslide susceptibility. Geomorphology 80(3):178–198

Guo CB, Montgomery DR, Zhang YS, Wang K, Yang ZH (2015) Quantitative assessment of landslide susceptibility along the Xianshuihe fault zone, Tibetan Plateau, China. Geomorphology 248:93–110

Guzzetti F, Carrarra A, Cardinali M, Reichenbach P (1999) Landslide hazard evaluation: a review of current techniques and their application in a multi-scale study, Central Italy. Geomorphology 31:181–216

Huang RQ, Li WL (2008) Research on development and distribution rules of geohazards induced by wenchuan earthquake on 12th may, 2008. Chin J Rock Mech Eng 27(12):2585–2592 **(in Chinese)**

Huang R, Li Y, Qu K, Wang K (2013) Engineering geological assessment for route selection of railway line in geologically active area: a case study in China. J Mt Sci 10(4):495–508

Ilia I, Tsangaratos P (2016) Applying weight of evidence method and sensitivity analysis to produce a landslide susceptibility map. Landslides 13(2):379–397

Kanungo DP, Arora MK, Sarkar S, Gupta RP (2006) A comparative study of conventional, ANN black box, fuzzy and combined neural and fuzzy weighting procedures for landslide susceptibility zonation in Darjeeling Himalayas. Eng Geol 85(3):347–366

Kayastha P, Dhital MR, Smedt FD (2012) Landslide susceptibility mapping using the weight of evidence method in the Tinau watershed Nepal. Nat Hazards 63(2):479–498

Kumar A, Sharma RK, Bansal VK (2019) GIS-based comparative study of information value and frequency ratio method for landslide hazard zonation in a part of mid-Himalaya in Himachal Pradesh. Innov Infrastruct Solut 4(1):28

Laimer HJ (2017) Anthropogenically induced landslides—a challenge for railway infrastructure in mountainous regions. Eng Geol 222:92–101

Lan HX, Zhou CH, Wang LJ, Zhang HY, Li RH (2004) Landslide hazard spatial analysis and prediction using GIS in the Xiaojiang Watershed, Yunnan, China. Eng Geol 76:109–128

Lee S, Choi J (2004) Landslide susceptibility mapping using GIS and the weight-of-evidence model. Int J Geogr Inf Sci 18:789–814

Lee S, Pradhan B (2006) Probabilistic landslide risk mapping at Penang Island, Malaysia. J Earth Syst Sci 115(6):661–672

Lee S, Pradhan B (2007) Landslide hazard mapping at Selangor, Malaysia using frequency ratio and logistic regression models. Landslides 4(1):33–41

Lee S, Ryu JH, Won JS, Park HJ (2004) Determination and application of the weights for landslide susceptibility mapping using an artificial neural network. Eng Geol 71(3–4):289–302

Lee CT, Huang CC, Lee JF, Pan KL, Lin ML, Dong JJ (2008) Statistical approach to earthquake-induced landslide susceptibility. Eng Geol 100(1):43–58

Li BK, Diao GL, Zou LY (2014) Earthquake source parameters reviewing of the Mw 7.7 earthquake in the southeast of Langxian, Tibet, 1947. Seismol Geomagn Obs Res 35(1):85–91 (in Chinese)

Macciotta R, Hendry M, Martin CD (2016) Developing an early warning system for a very slow landslide based on displacement monitoring. Nat Hazards 81(2):887–907

Mehebub S, Haroon S (2017) Evaluating effectiveness of frequency ratio, fuzzy logic and logistic regression models in assessing landslide susceptibility: a case from Rudraprayag district, India. J Mt Sci 14(11):2150–2167

Mohammady M, Pourghasemi HR, Pradhan B (2012) Landslide susceptibility mapping at Golestan Province, Iran: a comparison between frequency ratio, Dempster–Shafer, and weights-of-evidence models. J Asian Earth Sci 61:221–236

Neuhauser B, Damm B, Terhorst B (2012) GIS-based assessment of landslide susceptibility on the base of the weights of evidence model. Landslides 9:511–528

Pandey VK, Sharma KK, Pourghasemi HR, Bandooni SK (2019) Sedimentological characteristics and application of machine learning techniques for landslide susceptibility modelling along the highway corridor Nahan to Rajgarh (Himachal Pradesh), India. CATENA 182:1–18

Park NW (2011) Application of Dempster–Shafer theory of evidence to GIS-based landslide susceptibility analysis. Environ Earth Sci 62(2):367–376

Pradhan B (2013) A comparative study on the predictive ability of the decision tree, support vector machine and neuro-fuzzy models in landslide susceptibility mapping using GIS. Comput Geosci 51(2):350–365

Pradhan B, Lee S (2010) Delineation of landslide hazard areas on Penang Island, Malaysia, by using frequency ratio, logistic regression, and artificial neural network models. Environ Earth Sci 60:1037–1054

Regmi NR, Giardino JR, Vitek JD (2010) Modeling susceptibility to landslides using the weight of evidence approach: Western Colorado, USA. Geomorphology 115(1–2):172–187

Regmi AD, Devkota KC, Yoshida K, Pradhan B, Pourghasemi HR, Kumamoto T, Akgun A (2014) Application of frequency ratio, statistical index, and weights-of-evidence models and their comparison in landslide susceptibility mapping in Central Nepal Himalaya. Arab J Geosci 7(2):725–742

Saponaro A, Pilz M, Wieland M, Bindi D, Moldobekov B, Parolai S (2015) Landslide susceptibility analysis in data-scarce regions: the case of Kyrgyzstan. Bull Eng Geol Environ 74(4):1117–1136

Sarkar S, Kanungo DP, Patra AK, Kumar P (2008) GIS based spatial data analysis for landslide susceptibility mapping. J Mt Sci 5(1):52–62

Sarro R, Riquelme A, García-Davalillo JC, Mateos RM, Tomás R, Pastor JL, Cano M, Herrera G (2018) Rockfall simulation based on uav photogrammetry data obtained during an emergency declaration: application at a cultural heritage site. Remote Sens 10(12):1923

Sciarra M, Coco L, Urbano T (2017) Assessment and validation of GIS-based landslide susceptibility maps: a case study from Feltrino stream basin (Central Italy). Bull Eng Geol Environ 76(2):437–456

Shao CR, You HC, Cao ZQ, Wang CY, Tang FT, Zhang DC, Lou H, Xu GY, Chang LJ, Yang QY, Mei D, Xie P, Yu G (2008) Tectonic characteristics and seismic activities of Yaluzangbu Grand Canyon, Tibet, China. Technol Earthq Disaster Prev 242(1):134–145 (in Chinese)

Sujatha ER, Rajamanickam GV, Kumaravel P (2012) Landslide susceptibility analysis using Probabilistic Certainty Factor Approach: a case study on Tevankarai stream watershed, India. J Earth Syst Sci 121(5):1337–1350

Sun D, Wang DY (2011) Structure features of the middle Yarlung Zangbo suture zone and a new knowledge of its genetic model. Acta Geol Sin 85(1):56–65 (in Chinese)

Tangestani MH (2009) A comparative study of Dempster–Shafer and fuzzy models for landslide susceptibility mapping using a GIS: an experience from Zagros Mountains, SW Iran. J Asian Earth Sci 35(1):66–73

Thiery Y, Malet JP, Sterlacchini S, Puissant A, Maquaire O (2007) Landslide susceptibility assessment by bivariate methods at large scales: Application to a complex mountainous environment. Geomorphology 92(1–2):38–59

Thiery Y, Maquaire O, Fressard M (2014) Application of expert rules in indirect approaches for landslide susceptibility assessment. Landslides 11(3):1–14

Tien Bui D, Pradhan B, Lofman O, Revhaug I, Dick OB (2012) Landslide susceptibility assessment in the Hoa Binh province of Vietnam: a comparison of the Levenberg–Marquardt and Bayesian regularized neural networks. Geomorphology 171–172:12–19

Varnes OJ (1978) Slope movements, type and processes. In: Schuster RL, Krizek RJ (eds) Landslide analysis and control. Transportation Research Board National Academy Sciences, Washington, DC, pp 11–33 (Special report 176)

van Westen CJ, Rengers N, Soeters R (2003) Use of geomorphological information in indirect landslide susceptibility assessment. Nat Hazards 30:399–419

Wu RA, Guo CB, Du YB, Wang K, Du GL (2017) Research on geohazard developing characteristics in Jiacha to Langxian section of Sichuan–Tibet railway. Geoscience 31(5):956–964 (in Chinese)

Xu C, Xu XW, Yuan HL, Tan XB, Yu GH, Dai FC (2012) The 2010 Yushu earthquake triggered landslide hazard mapping using GIS and weight of evidence modeling. Environ Earth Sci 66(6):1603–1616

Yalcin A, Reis S, Aydinoglu AC, Yomralioglu T (2011) A GIS-based comparative study of frequency ratio, analytical hierarchy process, bivariate statistics and logistics regression methods for

landslide susceptibility mapping in Trabzon, NE Turkey. CATENA 85:274–287

Yilmaz I (2010) Comparison of landslide susceptibility mapping methodologies for Koyulhisar, Turkey: conditional probability, logistic regression, artificial neural networks, and support vector machine. Environ Earth Sci 61:821–836

Youssef AM, Pourghasemi HR, El-Haddad BA, Dhahry BK (2016) Landslide susceptibility maps using different probabilistic and bivariate statistical models and comparison of their performance at Wadi Itwad Basin, Asir Region, Saudi Arabia. Bull Eng Geol Environ 75(1):1–25

Zhang Y, Yang Z, Guo C, Wang T, Wang D, Du G (2017) Predicting landslide scenes under potential earthquake scenarios in the Xianshuihe fault zone, Southwest China. J Mt Sci 14(7):1262–1278

Zhou D (2011) Comprehensive assessment the risk of the geological disasters to railway from Linzhi to Lhasa—taking the railway from to Langxian for example. Master's thesis from Chengdu University of technology (**in Chinese**)